Chapter 5

The scaling law of human travel - A message from George

Dirk Brockmann and Lars Hufnagel
Max Planck Institute for Dynamics and Self-Organziation
Bunsenstr.10
37073 Göttingen, Germany
E-mail: brockmann@ds.mpg.de

The dispersal of individuals of a species is the key driving force of various spatiotemporal phenomena which occur on geographical scales. It can synchronize populations of interacting species, stabilize them, and diversify gene pools.[1–3] The geographic spread of human infectious diseases such as influenza, measles and the recent severe acute respiratory syndrome (SARS) is essentially promoted by human travel which occurs on many length scales and is sustained by a variety of means of transportation[4–8]. In the light of increasing international trade, intensified human traffic, and an imminent influenza A pandemic the knowledge of dynamical and statistical properties of human dispersal is of fundamental importance and acute.[7,9,10] A quantitative statistical theory for human travel and concomitant reliable forecasts would substantially improve and extend existing prevention strategies. Despite its crucial role, a quantitative assessment of human dispersal remains elusive and the opinion that humans disperse diffusively still prevails in many models.[11] In this chapter we will report on a recently developed technique which permits a solid and quantitative assessment of human dispersal on geographical scales.[12] The key idea is to infer the statistical properties of human travel by analysing the geographic circulation of individual bank notes for which comprehensive datasets are collected at online bill-tracking websites. The analysis shows that the distribution of traveling distances decays as a power law, indicating that the movement of bank notes is reminiscent of superdiffusive, scale free random walks known as Lévy flights.[13] Secondly, the probability of remaining in a small, spatially confined region for a time T is dominated by heavy tails which attenuate superdiffusive dispersal. We will show that the dispersal of bank notes can be described on many spatiotemporal scales by a two parameter continuous time random walk (CTRW) model to a surprising

accuracy. We will provide a brief introduction to continuous time random walk theory[14] and will show that human dispersal is an ambivalent, effectively superdiffusive process.

The notion of dispersal in ecology usually refers to the movement of individuals of a species in their natural environment.[1,3] The statistical properties of dispersal can be quantified by the dispersal curve $p_{\Delta t}(\Delta \mathbf{x})$. The dispersal curve reflects the relative frequency of geographic displacements $\Delta \mathbf{x}$ which are traversed within a given period of time Δt.* A large class of dispersal curves (for example, exponential, gaussian, stretched exponential) exhibit a characteristic length scale.[15] That is, when interpreted as the probability of finding a displacement of length $\Delta \mathbf{x}$, a length scale can be defined by the square root of second moment, i.e. $\sigma = \sqrt{\langle \Delta \mathbf{x}^2 \rangle}$. The existence of a typical length scale often justifies the description of dispersal in terms of diffusion equations on spatiotemporal scales larger than Δt and σ.[16] Because, if single displacements are sufficiently uncorrelated the probability density $W(\mathbf{x}, t)$ of having traversed a total displacement $\mathbf{x}$ after time t is a Gaussian which obeys Fick's second law:

$$\partial_t W = D\, \partial_x^2 W, \tag{5.1}$$

where $D = \sigma^2/\Delta t$ is the diffusion coefficient. This result is a consequence of the central limit theorem[17] and does not depend on the precise form of the short time dispersal curve as long as the variance $\langle \Delta x^2 \rangle$ is finite.

In population dynamical systems this type of diffusive dispersal is quite frequently combined with a reaction kinetic scheme which accounts for local interactions between various types of reacting agents, for example various species in predator-prey systems. Sometimes groups of individuals of a single species which interact are classified according to some criterion. For instance in the context of epidemiology a population is often classified according to their infective status.

In an approximation which neglects the intrinsic fluctuations of the underlying reaction kinetics one obtains for these systems reaction-diffusion equations, the most prominent example of which is the Fisher equation†,[18]

$$\partial_t u = \lambda u(1-u) + D\partial_x^2 u, \tag{5.2}$$

*In ecological literature, the term "dispersal" is commonly used in the context of the spatial displacement of individuals of a species between their geographical origin of birth and the location of their first breeding place, a process which occurs on time scales of the lifespan of the individuals. Here we use the term dispersal to refer to geographical displacements that occur on much shorter timescales of the order of days.

†also referred to as the Fisher-Kolmogorov-Petrovsky-Piscounov equation.

for the concentration $u(\mathbf{x}, t)$ of a certain class of individuals, a species etc. A paradigmatic system which naturally yields a description in terms of Eq. (5.2) and which has been used to describe to geographic spread of infectious diseases is the SIS-model in which a local population of N individuals segregates into the two classes of susceptible S who may catch a disease and infected I who transmit it. Transmission is quantified by the rate α and recovery by the rate β.[11] The reaction scheme could not be simpler:

$$S + I \xrightarrow{\alpha} 2I \qquad I \xrightarrow{\beta} S\,. \tag{5.3}$$

In the limit of large population size N the dynamics can be approximated by the set of differential equations

$$\partial_t S = -\alpha IS/N, \qquad \partial_t I = \alpha IS/N - \beta I. \tag{5.4}$$

Assuming that the number of individuals is conserved (i.e. $I(t)+S(t) = N$) and that disease transmission is more frequent than recovery ($\alpha > \beta$) one obtains for the rescaled relative number of infected $u(t) = \alpha I(t)/N(\alpha - \beta)$ a single ordinary differential equation (ODE) describing logistic growth:

$$\partial_t u = \lambda u(1 - u), \tag{5.5}$$

where $\lambda = \alpha - \beta$. If, additionally reactants are free to move diffusively one obtains Eq. (5.2) for the dynamics of the relative number of infected $u(\mathbf{x}, t)$ as a function of position and time.

The popularity and success of the Fisher-equation and similar equations in the field of theoretical biology can be ascribed to some extent to the fact that they possess propagating front solutions and that qualitatively similar patterns were observed in historic pandemics. The most prominent example is the bubonic plague pandemic of the 14th century which crossed the European continent as a wave within three years at an approximate speed of a few kilometers per day. Aside from factors which are known to play a role, such as social contact networks, age structure, inhomogeneities in local populations and inhomogeneities in the geographic distribution of the population, there is something fundamentally wrong with the diffusion assumption on which this class of equations is based upon. Humans (with the exception maybe of nomads) do not and never did diffuse on timescales of their lifespan. A simple argument can be given why this cannot be so. For a diffusion process the expected time for returning to the point of origin is infinite[19] (despite the fact that in spatial dimensions $d \leq 2$ the probability of returning is unity). It would not make much sense to have a

home if the expected time to return to it is infinite. However, in the context of the geographic spread of infectious diseases it does at times make sense to employ reaction-diffusion equations. That is because the position of what is passed from human to human, i.e. the pathogens, is what matters and not the position of single host individuals. Unlike humans, pathogens are passed from human to human and opposed to humans pathogens have no inclination of returning. They disperse diffusively and a description in terms of reaction-diffusion dynamics is justified, see Fig. (5.1).

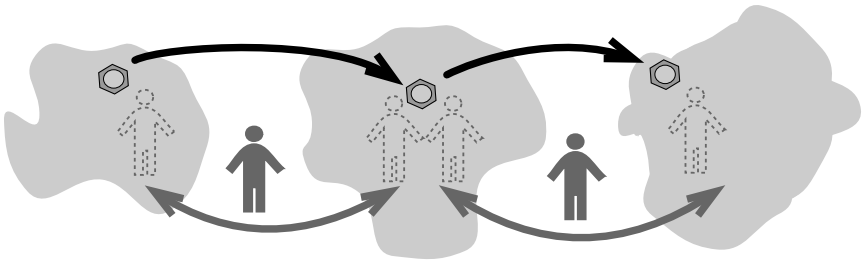

Fig. 5.1. Human travel and the dispersal of pathogens. The gray areas depict home ranges of individuals. By virtue of overlapping home ranges and inter-homerange travel an infectious disease spreads in space. Although humans travel back and forth between home ranges, pathogens spread continuously in space.

Recently the notion of long distance dispersal (LDD) has been established in dispersal ecology,[20] taking into account the observations that a number of dispersal curves exhibit long, algebraic tails which forbid the identification of a typical scale and thus a description of dispersal phenomena based on diffusion equations. If, for instance, the probability density of traversing a distance r in a given period of time Δt decreases according to

$$p_{\Delta t}(r) \sim \frac{1}{r^{1+\beta}} \tag{5.6}$$

with a tail exponent $\beta < 2$, the variance of the displacement magnitude is infinite and consequently no typical length scale can be identified. Power-law distributions of this type are abundant in nature. Meteorite sizes, city sizes, income and the number of species per genus follow power-law distributions.[21]

In physics, random walk processes with a power-law single-step distribution are known as Lévy flights.[14,22–24] Due to the lack of scale in the single steps, Lévy flights are qualitatively different from ordinary random

walks. Unlike ordinary random walks the position $\mathbf{X}_N = \sum_n^N \Delta\mathbf{x}_n$ after N steps $\Delta\mathbf{x}_n$ scales with the number of steps according to

$$\mathbf{X}_N \sim N^{1/\beta} \tag{5.7}$$

with $\beta < 2$. Thus, Lévy flights disperse "faster" than the ordinary $N^{1/2}$ behavior exhibited by ordinary random walks; Lévy flights are superdiffusive. Furthermore, the probability density for the position $p(\mathbf{x}, N)$ for Lévy flights behaves asymptotically as

$$p(\mathbf{x}, N) \sim N^{-D/\beta} L_\beta \left(\mathbf{x}/N^{1/\beta}\right) \tag{5.8}$$

where D is the spatial dimension and the function L_β is known as the symmetric Lévy-stable law of index β. This limiting function is a generalization of the ordinary Gaussian and can be expressed by its Fourier-transform

$$L_\beta(\mathbf{z}) = \frac{1}{(2\pi)^{D/2}} \int \mathrm{d}\mathbf{k}\, e^{-i\mathbf{z}\cdot\mathbf{k} - |\mathbf{k}|^\beta}. \tag{5.9}$$

The limiting value $\beta = 2$ corresponds to the Gaussian, the limiting function for ordinary random walks. The lack of scale in a Lévy flight, its superdiffusive nature and the geometrical difference between Lévy flights and ordinary random walks are illustrated in figure 5.2. Lévy flights, and superdiffusive random motion were observed in a variety of physical and biological systems, ranging from transport in chaotic systems[25] and turbulent flows,[26] to foraging patterns of wandering albatrosses[27] and spider monkeys.[28]

Nowadays, humans travel on many spatial scales, ranging from a few to thousands of kilometres over short periods of time. The direct quantitative assessment of human movements, however, is difficult, and a statistically reliable estimate of human dispersal comprising all spatial scales does not exist. Contemporary models for the spread of infectious diseases across large geographical regions have to make assumptions on human travel. The notion that humans travel short distances more frequently than long ones is typically taken into account. Yet, the precise ratio of the frequency of short trips and the frequency of long trips is not known and must be assumed. Furthermore, it is generally agreed upon that human travel, being a complex phenomenon, adheres to complex mathematical rules with a lot of detail.

Recently, it was shown that the global spread of SARS in 2003 can be reproduced by a model which takes into account nearly the entire civil

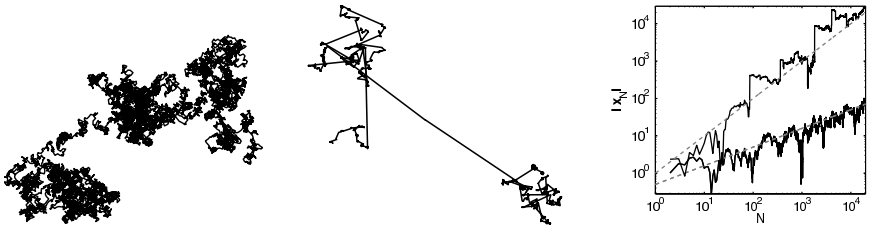

Fig. 5.2. Ordinary random walks and Lévy flights. *Left:* The trajectory of an ordinary random walk in two dimensions, equivalent to Brownian motion on large spatiotemporal scales. *Middle:* Unlike Brownian motion, the trajectory of the two-dimensional Cauchy-process, indexprocess!Cauchy i.e. a Lévy flight with Lévy exponent $\beta = 1$ exhibits local clustering interspersed with long distance jumps. *Right:* The distance $|\mathbf{X}_N|$ from the starting point $\mathbf{X}_0 = 0$ of an ordinary random walk (lower trajectory) and a Lévy flight ($\beta = 1$, upper trajectory) as a function of step number N. The dashed lines indicate the scaling $N^{1/2}$ and $N^{1/\beta}$ respectively. Clearly, the Lévy flight is superdiffusive.

aviation network.[7,10] Despite the high degree of complexity of aviation traffic, the strong heterogeneity of the network yields an unexpectedly narrow range of fluctuations, supporting the idea that reliable forecasts of the geographic spread of disease is possible. Although the model successfully accounts for the geographic spread on global scales, it cannot account for the spread on small and intermediate spatial scales. To this end a comprehensive knowledge of human travel on scales ranging from a few to a few thousand kilometers is necessary. However, collecting comprehensive traffic data for all means of human transportation involved is difficult of not impossible.

In a recent study,[12,29] we circumvent the technical difficulty of measuring human travel directly by using the dispersal of bank notes in the United States. The key idea of the project is to use bank note dispersal as a proxy for human travel. We collected data from the online bill-tracking website www.wheresgeorge.com. The idea of this internet game, which was initiated in 1998 by Hank Eskin, is simple. Individual bank notes are marked by registered users and brought into circulation. When people come into possession of such marked bank notes, they can register at the website and report their current location and return the bank note into circulation. Thus, registered users can monitor the geographical dispersal of their money. Meanwhile, over 80 millions dollar bills have been registered and over 3 million users participate in the game. As bank notes are primarily transported by traveling humans, we were able to infer the sta-

tistical properties of human travel from the dispersal of bank notes with high spatio-temporal precision.

Our analysis of human movement is based on the trajectories of a subset of 464,670 dollar bills obtained from the website. We analyzed the dispersal of bank notes in the United States, excluding Alaska and Hawaii. The core data consists of 1,033,095 reports to the website. From these reports we calculated the geographical displacements $r = |\mathbf{x}_2 - \mathbf{x}_1|$ between a first ($\mathbf{x}_1$) and secondary ($\mathbf{x}_2$) report location of a bank note and the elapsed time T between successive reports. The pairs of datapoints $\{r_i, T_i\}$ represent our core dataset, from which the probability density function (pdf) $W(r,t)$ of having traveled a distance r after a time t can be estimated.

In order to illustrate qualitative features of bank note trajectories, Fig. 5.3 depicts short time trajectories ($T < 14$ days) originating from three major cities (Seattle, WA, New York, NY, Jacksonville, FL). Succeeding their initial entry, the majority of bank notes are reported next in the vicinity of the initial entry location, i.e. $r < 10$ km (Seattle: 52.7%, New York: 57.7% Jacksonville: 71.4%). However, a small yet considerable fraction is reported beyond a distance of 800 km (Seattle: 7.8%, New York: 7.4%, Jacksonville: 2.9%).

From a total of $N = 20,540$ short time displacements we measured the probability density $p(r)$ of traversing a distance r in a time interval δT between one and four days. The result is depicted in Fig. 5.4. A total of $14,730$ (i.e. a fraction $Q = 0.71$) secondary reports occur outside a short range radius $L_{\min} = 10\,\mathrm{km}$. Between $L_{\min}$ and the approximate average east-west extention of the United States $L_{\max} \approx 3,200\,\mathrm{km}$ $p(r)$ exhibits power law behavior $p(r) \sim r^{-(1+\beta)}$ with an exponent $\beta = 0.59 \pm 0.02$. For $r < L_{\min}$, $p(r)$ increases linearly with r which implies that displacements are distributed uniformly inside the disk $|\mathbf{x}_2 - \mathbf{x}_1| < L_{\min}$.

One might speculate whether the observed lack of scale in $p(r)$ is not a dynamic property of dispersal but rather imposed by the substantial spatial inhomogeneity of the United states. For instance, the probability of traveling a distance r might depend strongly on static properties such as the local population density. In order to test this hypothesis, we have measured $p(r)$ for three classes of initial entry locations: highly populated metropolitan areas (191 locations, local population $N_{\mathrm{loc}} > 120,000$), cities of intermediate size ($1,544$ locations, local population $120,000 > N_{\mathrm{loc}} > 22,000$), and small towns ($23,640$ locations, local population $N_{\mathrm{loc}} < 22,000$) comprising 35.7 %, 29.1 % and 25.2 % of the entire population of the United States, respectively. Fig. 5.4 also depicts $p(r)$ for these classes. Despite systematic

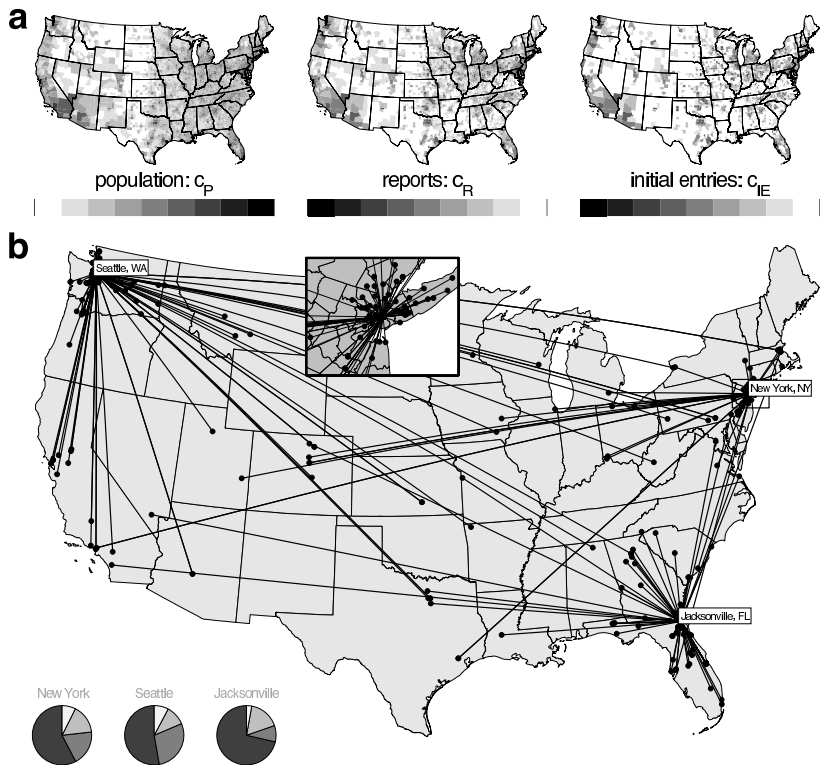

Fig. 5.3. Dispersal of bank notes on geographical scales. ***a:*** Relative logarithmic densities of population ($c_{\rm P} = \log_{10} \rho_{\rm P} / \langle \rho_{\rm P} \rangle$), reports ($c_{\rm R} = \log_{10} \rho_{\rm R} / \langle \rho_{\rm R} \rangle$) and initial entry ($c_{\rm IE} = \log_{10} \rho_{\rm IE} / \langle \rho_{\rm IE} \rangle$) as functions of geographical coordinates. The shades of gray encode the densities relative to the nation-wide averages (3,109 counties) of $\langle \rho_{\rm P} \rangle = 95.15$, $\langle \rho_{\rm R} \rangle = 0.34$ and $\langle \rho_{\rm IE} \rangle = 0.15$ individuals, reports and initial entries per km^2, respectively. ***b:*** Short time trajectories of bank notes originating from three different places. Tags indicate initial, symbols secondary report locations. Lines represent short time trajectories with traveling time $T < 14$ days. The inset depicts a close-up of the New York area. Pie charts indicate the relative number of secondary reports coarsely sorted by distance. The fractions of secondary reports that occurred at the initial entry location (dark), at short ($0 < r < 50$ km), intermediate ($50 < r < 800$ km) and long ($r > 800$ km) distances are ordered by increasing brightness. The total number of initial entries are $N = 524$ (Seattle), $N = 231$ (New York), $N = 381$ (Jacksonville).

deviations for short distances, all distributions exhibit an algebraic tail with the same exponent $\beta \approx 0.6$. This confirms that the observed power-law is an intrinsic and universal property of dispersal, the first experimental evidence that bank note trajectories are reminiscent of Lévy flights and that

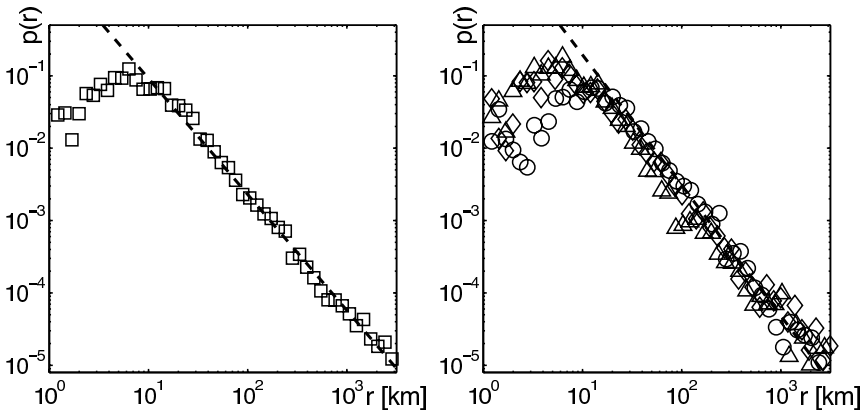

Fig. 5.4. Quantitative analysis of bank note dispersal. *Left:* The short time dispersal kernel. The measured probability density function $p(r)$ of traversing a distance r in less than $T = 4$ days is depicted by squares. It is computed from an ensemble of $20,540$ short time displacements. The dashed black line indicates a power law $p(r) \sim r^{-(1+\beta)}$ with an exponent of $\beta = 0.59$. *Right:* $p(r)$ for three classes of initial entry locations (black triangles for metropolitan areas, diamonds for cities of intermediate size, and circles for small towns).

dispersal is superdiffusive.

However, the situation is more complex. If we assume that the dispersal of bank notes can be described by a Lévy flight with a short time probability distribution $p(r)$ as depicted in Fig. 5.4, we can estimate the time $T_{\rm eq}$ for an initially localized ensemble of bank notes to reach the stationary distribution (maps in Fig. 5.3). We assume that the Lévy flight evolves in a two-dimensional region of linear extent L. Furthermore we assume that the single step distribution for a vectorial displacement $\mathbf{x}$ of the random walk can be approximated by

$$p_{\Delta t}(\mathbf{x}) = (1 - Q)\delta(\mathbf{x}) + Q\, f_{\delta L}(\mathbf{x}). \tag{5.10}$$

Here Δt denotes the typical time between single steps, Q the fraction of walkers which jump a distance $d > \delta L$ and $(1 - Q)$ the fraction which remains in a disk defined by $|\mathbf{x}| \leq \delta L$. The function $f_{\delta L}(\mathbf{x})$ comprises the power-law in the single steps, characteristic for Lévy flights:

$$f_{\delta L}(\mathbf{x}) = C\, \delta L^{\beta} |\mathbf{x}|^{-(2+\beta)} \qquad |\mathbf{x}| \geq \delta L. \tag{5.11}$$

Inserting this into Eq. (5.10) one obtains that $f_{\delta L}(\mathbf{x})$ is normalized to unity and that the normalization constant C is independent of the microscopic length δL. The Fourier-transform of $p(\mathbf{x})$ is given by $\tilde{p}(\mathbf{k}) = (1 - Q) +$

$Q\tilde{f}_{\delta L}(\mathbf{k})$.The Fourier-transform of the probability density function $W_N(\mathbf{x})$ of the walker being located at a position $\mathbf{x}$ after N steps can be computed in terms of $\tilde{p}(\mathbf{k})$ according to

$$\tilde{W}_N(\mathbf{k}) = \tilde{p}(\mathbf{k})^N \approx \left(1 - Q\delta L^\beta |\mathbf{k}|^\beta\right)^N \approx e^{-QN\,|\delta L\,\mathbf{k}|^\beta}. \tag{5.12}$$

The relaxation time in a confined region is provided by the lowest mode $k_{\min} = L/2\pi$. Inserted into (5.12) with $N = t/\Delta t$ one obtains

$$T_{\rm eq} \approx \delta T/Q\,(L/2\pi\delta L)^\beta = 68\,\text{days}. \tag{5.13}$$

Thus, after $2-3$ months bank notes should have reached the equilibrium distribution. Surprisingly, the long time dispersal data does not reflect a relaxation within this time.

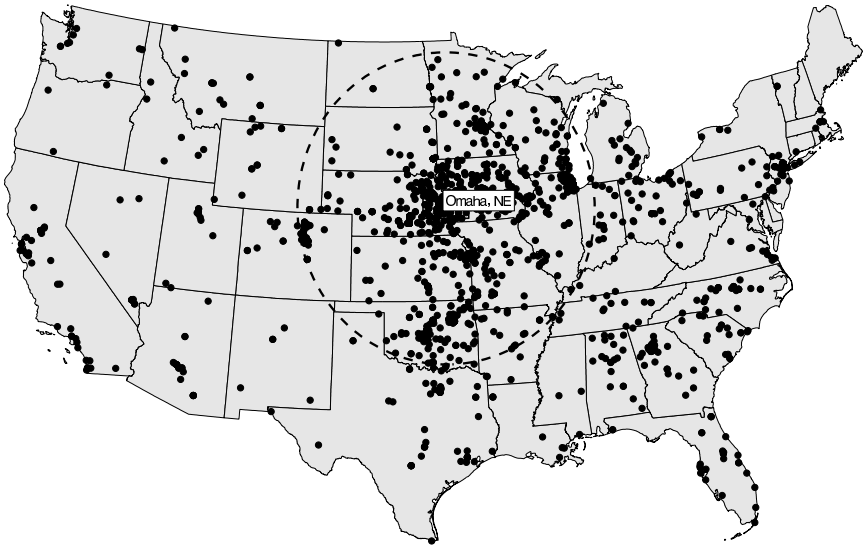

Fig. 5.5. Long time dispersal of bank notes with an initial entry in Omaha, NE. Points denote the location of the second report. Each bill travelled for a time greater than 100 days, with an average of 289 days. The dashed circle indicates the distance of 800 km from Omaha.

Fig. 5.5 shows secondary reports of bank notes with initial entry at Omaha, NE which have dispersed for times $T > 100\,$days (with an average time $\langle T\rangle = 289$ days). Only 23.6% of the bank notes traveled farther than 800 km, the majority of 57.3% travelled an intermediate distance $50 < r < 800\,$km and a relatively large fraction of 19.1% remained within a radius

of 50 km even after an average time of nearly one year. From Eq. 5.13 a much higher fraction of bills is expected to reach the metropolitan areas of the West Coast and the New England states after this time. This indicates that the simple Lévy flight picture for dispersal is incomplete. What causes this attenuation of the dispersal?

A possible explanations of this effect is a strong impact of the spatial inhomogeneity of the system. For instance, the typical time of rest in a geographical region might depend on local properties such as the population density. People might be less likely to leave large cities than e.g. suburban areas.

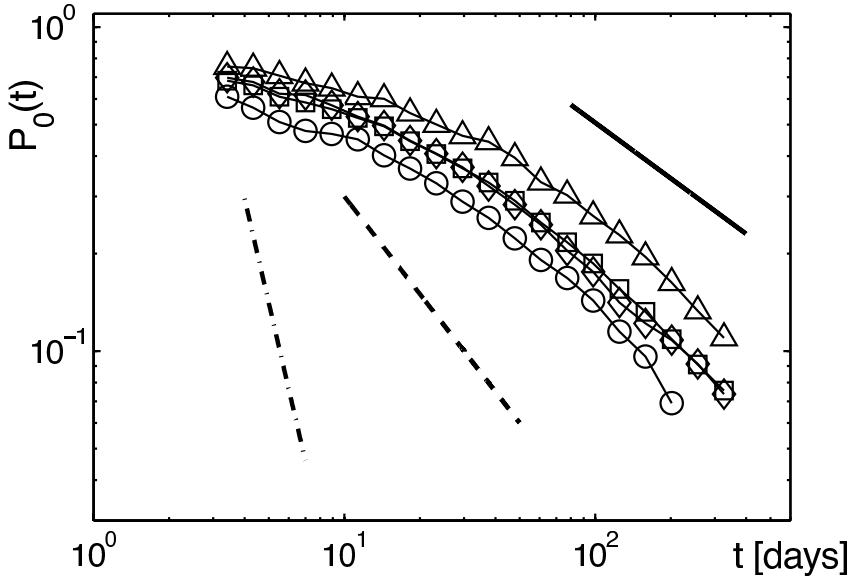

Fig. 5.6. The relative proportion $P_0(t)$ of secondary reports within a short radius ($r_0 =$ 20 km) of the initial entry location as a function of time. Squares depict $P_0(t)$ averaged over 25,375 initial entry locations. Triangles, diamonds, and circles show $P_0(t)$ for the same classes as in Fig 5.4. All curves decrease asymptotically as $t^{-\xi}$ with an exponent $\xi = 0.6 \pm 0.03$ indicated by the solid line. Ordinary diffusion in two dimensions predicts an exponent $\xi = 1$ (black dashed line). Lévy flight dispersal with an exponent $\beta = 0.6$ as suggested by the short time dispersal kernel (Fig. 5.4) predicts an even steeper decrease, $\xi = 3.33$ (dot-dashed line).

In order to address this issue we investigated the relative proportion $P_0^i(t)$ of bank notes which are reported again in a small (20 km) radius of the initial entry location i as a function of time (Fig. 5.6). The quantity

$P_0^i(t)$ estimates the probability for a bank note of being reported at the initial location at time t a second time. In order to obtain reliable estimates we averaged this quantity over the above classes of initial entry locations (e.g. metropolitan areas, cities of intermediate size and small towns): For all classes we found the asymptotic behavior $P_0(t) \sim A\, t^{-\eta}$ with an exponent $\eta \approx 0.60 \pm 0.03$ and a coefficient A. The observed difference in values of the coefficient A reflects the impact of the inhomogeneity of the system, i.e. bank notes are more likely to remain in highly populated areas. The exponent η, however, is approximately the same for all classes which indicates that waiting time and dispersal characteristics are universal and do not depend significantly on external factors such as the population density. Notice that for a pure two dimensional Lévy flight with index β the function $P_0(t)$ scales as $t^{-\eta}$ with $\eta = 2/\beta$. For $\beta \approx 0.6$ (as put forth by Fig. 5.4) this implies $\eta \approx 3.33$,[19] i.e. a five fold steeper decrease than observed, which clearly shows that dispersal cannot be described by a pure Lévy flight model. The measured decay is even slower than the decay exhibited by ordinary two-dimensional diffusion ($\eta = 1$[19]). This is very puzzling.

What could be the reason behind the attenuation of dispersal? One way of slowing down dispersal are long periods of rest. In as much as an algebraic tail in the spatial displacements yields superdiffusive behavior, a tail in the probability density $\psi(\Delta t)$ for times Δt between successive spatial displacements of an ordinary random walk can lead to subdiffusion. For instance, if $\psi(\Delta t) \sim \Delta t^{-(1+\alpha)}$ with $\alpha < 1$, the position of an ordinary random walker scales according to $X(t) \sim t^{2/\alpha}$.[14] In combination with a power-law in the spatial displacements this ambivalence yields a competition between long jumps and long rests and can be responsible for the attenuation of dispersal.[30]

We test this idea of an antagonistic interplay between scale free displacements and waiting times within the framework of the continuous time random walk (CTRW) introduced by Montroll and Weiss.[31] A CTRW consists of a succession of random displacements $\Delta\mathbf{x}_n$ and random waiting times Δt_n each of which is drawn from a corresponding probability density function $p(\Delta\mathbf{x})$ and $\psi(\Delta t)$. Spatial and temporal increments are assumed to be statistically independent. Furthermore, we assume that the spatial distribution is symmetric, i.e. $p(\Delta\mathbf{x}) = p(|\Delta\mathbf{x}|)$, and since the temporal increments are all positive $\psi(\Delta t)$ is single sided. After N iterations the position of the walker and the elapsed time is given by $\mathbf{X}_N = \sum_n \Delta\mathbf{x}_n$ and $T_N = \sum_n \Delta t_n$. The quantity of interest is the position $\mathbf{X}(t)$ after time

t. The probability density $W(\mathbf{x}, t)$ for this process can be computed in a straightforward fashion[14] and can be expressed in terms of the spatial distribution $p(\Delta\mathbf{x})$ and the temporal distribution $\psi(\Delta t)$. The Fourier-Laplace transform of $W(\mathbf{x}, t)$ is given by

$$\tilde{W}(\mathbf{k}, u) = \frac{1 - \tilde{\psi}(u)}{u\left(1 - \tilde{\psi}(u)\,\tilde{p}(\mathbf{k})\right)}, \tag{5.14}$$

where $\tilde{\psi}(u)$ and $\tilde{p}(\mathbf{k})$ denote the Laplace- and Fourier transform of $\phi(\Delta t)$ and $p(\Delta\mathbf{x})$, respectively. The probability density $W(\mathbf{x}, t)$ is then obtained by inverse Laplace-Fourier transform

$$W(\mathbf{x}, t) = \frac{1}{(2\pi)^3 i}\int_{c-i\infty}^{c+i\infty} \mathrm{d}u \int \mathrm{d}\mathbf{k}\, e^{ut - ikx}\tilde{W}(\mathbf{k}, u). \tag{5.15}$$

When both, the variance of the spatial steps $\left\langle(\Delta\mathbf{x})^2\right\rangle = \sigma^2$ and the expectation value $\langle\Delta t\rangle = \tau$ of the temporal increments exist the Fourier- and Laplace transform of $p(\Delta\mathbf{x})$ and $\psi(\Delta t)$ are given by

$$\tilde{p}(\mathbf{k}) = 1 - \sigma^2\mathbf{k}^2 + \mathcal{O}(\mathbf{k}^4) \tag{5.16}$$

$$\tilde{\psi}(u) = 1 - \tau u + \mathcal{O}(u^2), \tag{5.17}$$

for small arguments, which yield the asymptotics of the process. Inserted into Eq. (5.14) and employing inversion (5.15) one obtains $W(\mathbf{x}, t) = (2\pi Dt)^{-1}e^{-\mathbf{x}^2/2Dt}$ in this limit with $D = \sigma^2/\tau$. Thus, whenever $\left\langle(\Delta\mathbf{x})^2\right\rangle$ and $\langle\Delta t\rangle$ are finite a CTRW is asymptotically equivalent to ordinary Brownian motion.

The situation is drastically different, when both, $p(\Delta\mathbf{x})$ and $\psi(\Delta t)$ exhibit algebraic tails of the form

$$p(\Delta\mathbf{x}) \sim \frac{1}{|\Delta x|^{2+\beta}} \qquad 0 < \beta < 2 \quad \text{and} \quad \phi(\Delta t) \sim \frac{1}{\Delta t^{1+\alpha}} \qquad 0 < \alpha < 1 \tag{5.18}$$

In this case one obtains for the asymptotic of $\tilde{p}(\mathbf{k})$ and $\tilde{\psi}(u)$:

$$\tilde{p}(\mathbf{k}) = 1 - D_\beta|\mathbf{k}|^\beta + \mathcal{O}(k^2) \tag{5.19}$$

$$\tilde{\psi}(u) = 1 - D_\alpha u^\alpha + \mathcal{O}(u). \tag{5.20}$$

Inserted into (5.14) yields the solution for the process in Fourier-Laplace space:

$$\tilde{W}_{\alpha,\beta}(\mathbf{k}, u) = \frac{u^{-1}}{1 + D_{\alpha,\beta}|\mathbf{k}|^\beta/u^\alpha}, \tag{5.21}$$

where the constant $D_{\alpha,\beta} = D_\beta/D_\alpha$ is a generalized diffusion coefficient. After inverse Laplace transform the solution in $(\mathbf{x}, t)$ coordinates reads:

$$W(\mathbf{x}, t) = \frac{1}{2\pi} \int \mathrm{d}\mathbf{k}\, e^{-i\mathbf{k}x} E_\alpha(-D_{\alpha,\beta}|\mathbf{k}|^\beta t^\alpha). \tag{5.22}$$

Here, E_α is the Mittag-Leffler function defined by

$$E_\alpha(z) = \sum_{n=0}^{\infty} \frac{z^n}{\Gamma(1+\alpha n)} \tag{5.23}$$

which is a generalization of the exponential function to which it is identical for $\alpha = 1$. The integrand $E_\alpha(-D_{\alpha,\beta}|\mathbf{k}|^\beta t^\alpha)$ is the characteristic function of the process. As it is a function of $\mathbf{k}t^{\alpha/\beta}$, the probability density $W(\mathbf{x}, t)$ can be expressed as

$$W(\mathbf{x}, t) = t^{-2\alpha/\beta} L_{\alpha,\beta}\left(\mathbf{x}/t^{\alpha/\beta}\right) \tag{5.24}$$

in which the function $L_{\alpha,\beta}(\mathbf{z}) = (2\pi)^{-1} \int \mathrm{d}\mathbf{k}\, E_\alpha(-|\mathbf{k}|^\beta - i\mathbf{k}\mathbf{z})$ is a universal scaling function which is characteristic for the process and depends on the two exponents α and β only. Most importantly, one can extract the spatio-temporal scaling of the ambivalent process from (5.22):

$$X(t) \sim t^{\alpha/\beta}. \tag{5.25}$$

The ratio of the exponents α/β resembles the interplay between sub- and superdiffusion. For $\beta < 2\alpha$ the ambivalent CTRW is effectively superdiffusive, for $\beta > 2\alpha$ effectively subdiffusive. For $\beta = 2\alpha$ the process exhibits the same scaling as ordinary Brownian motion, despite the crucial difference of infinite moments and a non-Gaussian shape of the probability density $W(\mathbf{x}, t)$. The function $W(\mathbf{x}, t)$ is a probability density for the vectorial displacements $\mathbf{x}$. From Eqs. (5.22) and (5.24) we can compute the probability density $W_r(r, t)$ for having traveled the scalar distance $r = |\mathbf{x}|$ by integration over all angles:

$$W_r(r, t) = t^{-\alpha/\beta} \tilde{L}_{\alpha,\beta}\left(r/t^{\alpha/\beta}\right), \tag{5.26}$$

with a universal scaling function $\tilde{L}_{\alpha,\beta}$ which can be expressed in terms of $L_{\alpha,\beta}$.

The validity of our model can be tested by estimating the empirical $W_r(r, t)$ from the entire dataset of a little over half a million displacements and elapse times and compare it to Eq. (5.26). The results of this analysis

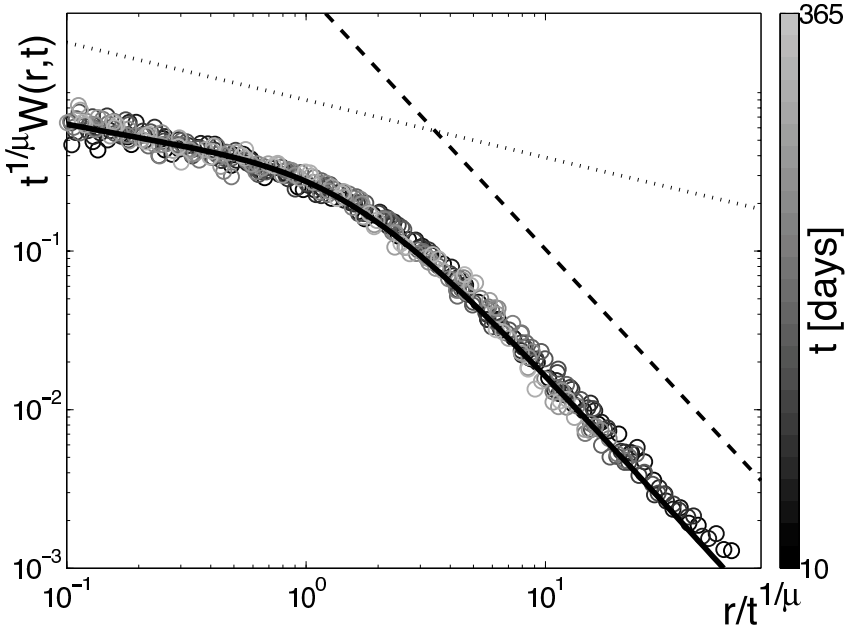

Fig. 5.7. The empirical radial probability density function $W_r(r,t)$ and theoretical scaling function $\tilde{L}_{\alpha,\beta}$. In order to extract scaling the function $W(r,t)$ is shown for various but fixed values of time t between 10 and 365 days as a function of $r/t^{1/\mu}$. For $\mu \approx 1.0$ the measured (circles) curves collapse on a single curve and the process exhibits universal scaling. The scaling curve represents the empirical limiting density F of the process. The asymptotic behavior for small (dotted line) and large (dashed line) arguments $y = r/t^{1/\mu}$ is given by $y^{-(1-\xi_1)}$ and $y^{-(1+\xi_2)}$, respectively, with estimated exponents $\xi_1 = 0.63 \pm 0.04$ and $\xi_2 = 0.62 \pm 0.02$. According to the our model these exponents must fullfill $\xi_1 = \xi_2 = \beta$ where β is the exponent of the asymptotic short time dispersal kernel (Fig. 5.4), i.e. $\beta \approx 0.6$. The superimposed solid line represents the scaling function predicted by our theory with spatial and temporal exponents $\beta = 0.6$ and $\alpha = 0.6$.

are compiled in Fig. 4.5. We can first address the question whether spatio-temporal scaling, i.e.

$$r(t) \sim t^{1/\mu} \tag{5.27}$$

is observed in the data with an empirically determined exponent μ. If this is so, then for the right choice of μ the quantity $t^{1/\mu}W_r(r,t)$ depends only on the argument $r/t^{1/\mu}$, that is

$$t^{1/\mu}W_r(r,t) = F\left(r/t^{1/\mu}\right), \tag{5.28}$$

with an empirical scaling function F. We found that for an exponent $\mu \approx 1$ and times between one week and one year, the relation (5.28) is indeed fullfilled and thus the dispersal of dollar bills exhibits scaling in this time window. Because the exponent $\mu < 2$, dispersal of bank notes is superdiffusive. Yet, μ is significantly larger than the tail exponent $\beta = 0.6$ of the short time dispersal kernel (Fig. 5.4), consistent with the idea that the process is slowed down by long periods of rest. Comparing with the spatio-temporal scaling promoted by the CTRW model $r(t) \sim t^{\alpha/\beta}$ a value of $\mu = 1$ would imply that temporal and spatial exponents are the same

$$\alpha = \beta. \tag{5.29}$$

Combined with the results obtained from the short time analysis yields

$$\alpha = \beta = 0.6. \tag{5.30}$$

A final test of the CTRW model is the comparison of the empirically observed scaling function F with the predicted scaling function $\tilde{L}_{\alpha,\beta}$ for the values of the exponents in Eq. (5.30). As depicted in Fig. 4.5 the asymptotic of the empirical curve is given by $y^{-(1-\xi_1)}$ and $y^{-(1+\xi_2)}$ for small and large arguments $y = r/t^{1/\mu}$, respectively. Both exponents fulfill $\xi_1 \approx \xi_2 \approx 0.6$. By series expansions one can compute the asymptotic of the CTRW scaling function $\tilde{L}_{\alpha,\beta}(y)$ which gives $y^{-(1-\beta)}$ and $y^{-(1+\beta)}$ for small and large arguments, respectively. Consequently, as $\beta \approx 0.6$ the theory agrees well with the observed exponents. For the entire range of y we computed $L_{\alpha,\beta}(y)$ by numeric integration for $\beta = \alpha = 0.6$ and superimposed the theoretical curve on the empirical one. The agreement is very good and strongly supports the CTRW model. In summary, our analysis gives solid evidence that the dispersal of bank notes can be accounted for by a simple random walk process with scale free jumps and scale free waiting times.

The question remains how the dispersal characteristics of bank notes carries over to the dispersal of humans and more importantly to the spread of human transmitted diseases. In this context one can safely assume that the power law with exponent $\beta = 0.6$ of the short time dispersal kernel for bank notes reflects the human dispersal kernel as only short times are considered. However, as opposed to bank notes humans tend to return from distant places they travelled to. This however, has no impact on the dispersal of pathogens which, much like bank notes, are passed from person to person and have no tendency to return. The issue of long waiting times is more subtle. One might speculate that the observed algebraic tail in waiting times of bank notes is a property of bank note dispersal alone.

Long waiting times may be caused by bank notes which exit the money tracking system for a long time, for instance in banks. However, if this were the case the inter-report time statistics would exhibit a fat tail. Analysing the inter-report time distribution we found an exponential decay which suggests that bank notes are passed from person to person at a constant rate. Furthermore, if we assume that humans exit small areas at a constant rate which is equivalent to exponentially distributed waiting times and that bank notes pass from person to person at a constant rate, the distribution of bank note waiting times would also be exponential in contrast to the observed power law. This reasoning permits no other conclusion than a lack of scale in human waiting time statistics.

Based on our analysis we conclude that the dispersal of bank notes and human transmitted diseases can be accounted for by a continuous time random walk process incorporating scale free jumps as well as long waiting time in between displacements. To our knowledge this is the first empirical evidence for such an ambivalent process in nature. Furthermore, the analysis permits a reliable estimate of the spatial and temporal exponents involved, i.e. $\beta \approx \alpha \approx 0.6$. We hope that our results will serve future models for the spread of human infectious disease as the key ingredient of dispersal, which can now be accounted for in a realistic way. We believe that these features, when combined with nonlinear epidemiological reaction kinetics, will lead to the emergence of novel types of spatiotemporal patterns.

References

1. J. Bullock, R. Kenward, and R. Hails, Eds., *Dispersal Ecology*. (Blackwell, Malden, Massachusetts, 2002).
2. J. D. Murray, *Mathematical Biology*. (Springer-Verlag Berlin Heidelberg New York, 1993).
3. J. Clobert, *Dispersal*. (Oxford Univ. Press, Oxford, 2001).
4. K. Nicholson and R. G. Webster, *Textbook of Influenza*. (Blackwell Publishing, Malden, MA, USA, 1998).
5. B. T. Grenfell, O. N. Bjornstadt, and J. Kappey, Travelling waves and spatial hierarchies in measles epidemics, *Nature*. **414**, 716, (2001).
6. M. J. Keeling, M. E. J. Woolhouse, D. J. Shaw, L. Matthews, M. Chase-Topping, D. T. Haydon, S. J. Cornell, J. Kappey, J. Wilesmith, and B. T. Grenfell, Dynamics of the 2001 uk foot and mouth epidemic: Stochastic dispersal in a heterogeneous landscape, *Science*. **294**, 813–817, (2001).
7. L. Hufnagel, D. Brockmann, and T. Geisel, Forecast and control of epidemics in a globalized world, *Proceedings of the National Academy of Sciences of the United States of America*. **101**(42), 15124–15129, (2004).

8. N. C. Grassly, C. Fraser, and G. P. Garnett, Host immunity and synchronized epidemics of syphilis across the united states, *Nature*. **433**(27), 417–421, (2005).
9. R. J. Webby and R. G. Webster, Are we ready for pandemic influenza?, *Science*. **302**, 1519–1522, (2003).
10. D. Brockmann, L. Hufnagel, and T. Geisel. Dynamics of modern epidemics. In eds. A. McLean, R. May, J. Pattison, and R. Weiss, *SARS: A Case Study in Emerging Infections*, pp. 81–92. Oxford University Press, Oxford, (2005).
11. R. M. Anderson, R. M. May, and B. Anderson, *Infectious Diseases of Humans : Dynamics and Control*. (Oxford Univ. Press, USA, 1992).
12. D. Brockmann, L. Hufnagel, and T. Geisel, The scaling laws of human travel, *Nature*. **439**(7075), 462–465, (2006).
13. M. Shlesinger, *Ly Flights and Related Topics in Physics*. (Springer Verlag, Berlin, 1995).
14. R. Metzler and J. Klafter, The random walk's guide to anomalous diffusion: a fractional dynamics approach, *Physics Reports-Review Section of Physics Letters*. **339**(1), 1–77, (2000).
15. M. Kot, M. A. Lewis, and P. vandenDriessche, Dispersal data and the spread of invading organisms, *Ecology*. **77**(7), 2027–2042, (1996).
16. C. W. Gardiner, *Handbook of Stochastic Methods*. (Springer Verlag, Berlin, 1985).
17. W. Feller, *An Introduction to Probability Theory and Its Application*. vol. I, (Wiley, New York, 1968).
18. R. A. Fisher, The wave of advance of advantageous genes, *Ann. Eugen.* (1937).
19. W. Feller, *An Introduction to Probability Theory and Its Application*. vol. II, (Wiley, New York, 1971).
20. R. Nathan, G. G. Katul, H. S. Horn, S. M. Thomas, R. Oren, R. Avissar, S. W. Pacala, and S. A. Levin, Mechanisms of long-distance dispersal of seeds by wind, *Nature*. **418**(6896), 409–413, (2002).
21. M. Schroeder, *Fractals, Chaos, Power Laws. Minutes from an Infinite Paradise*. (W. H. Freeman and Company, New York, 1991).
22. M. F. Shlesinger, G. M. Zaslavsky, and U. Frisch, Eds., *Ly flights and related Topics in Physics*. (Springer, Berlin, 1995).
23. D. Brockmann and T. Geisel, Levy flights in inhomogeneous media, *Physical Review Letters*. **90**(17), 170601, (2003). 673WT Times Cited:19 Cited References Count:17.
24. D. Brockmann and I. M. Sokolov, Levy flights in external force fields: from models to equations, *Chemical Physics*. **284**(1-2), 409–421, (2002).
25. T. Geisel, J. Nierwetberg, and A. Zacherl, Accelerated diffusion in josephson-junctions and related chaotic systems, *Physical Review Letters*. **54**(7), 616–619, (1985).
26. A. L. Porta, G. A. Voth, A. M. Crawford, J. Alexander, and E. Bodenschatz, Fluid particle accelaration in fully developed turbulance, *Nature*. **409**, 1017–1019, (2001).
27. G. M. Viswanathan, V. Afanasyev, S. V. Buldyrev, E. J. Murphy, P. A.

Prince, and H. E. Stanley, Levy flight search patterns of wandering albatrosses, *Nature*. **381**(6581), 413–415, (1996).
28. G. Ramos-Fernandez, J. L. Mateos, O. Miramontes, G. Cocho, H. Larralde, and B. Ayala-Orozco, Levy walk patterns in the foraging movements of spider monkeys (ateles geoffroyi), *Behavioral Ecology and Sociobiology*. **55**(3), 223–230, (2004).
29. M. F. Shlesinger, Follow the money, *Nature Physics*. **2**(2), 69–70, (2006).
30. M. F. Shlesinger, J. Klafter, and Y. M. Wong, Random-walks with infinite spatial and temporal moments, *Journal of Statistical Physics*. **27**(3), 499–512, (1982).
31. E. W. Montroll and G. H. Weiss, Random walks on lattices .2., *Journal of Mathematical Physics*. **6**(2), 167, (1965).